

# Oxide Ceramic Fibre Development at Fraunhofer Center HTL

Oxide ceramic fibres are required for reinforcement of metal matrix and ceramic matrix composites – especially in high temperature applications. Fraunhofer Center HTL/DE has been successfully developing customised oxide and non-oxide ceramic fibres for more than 20 years. In the field of oxide fibres, R&D work is focused on reinforcing fibres in the mullite-corundum system.



Fig. 1  
Oxide ceramic reinforcing fibres (l.), and CMC winding bodies (r.)

Oxide ceramic fibres are excellent candidates for the reinforcement of Metal Matrix Composites (MMC) and Ceramic Matrix Composites (CMC) due to their high strength, thermal and chemical stability, creep resistance, low density and shock resistance (Fig. 1). MMC have a significantly higher creep resistance than monolithic metal materials, the fibre reinforcement gives CMC a high damage tolerance and a quasi-ductile material behaviour. The advantage of oxide fibres compared to non-oxide ceramic fibres such as SiC is their inherent oxidation resistance. The ap-

#### Keywords

CFC fixtures, ceramic fibre, mullite fibre, alumina fibre, oxide ceramic fibre, reinforcing ceramic fibre

plications for MMC are for instance brake discs, brake lining carrier plates, connecting rods, bearings etc. in the automotive sector to reduce weight and increase wear properties. The applications of CMC are diverse and range from kiln furniture, flame tubes in oil or gas burners, brake discs to applications (i.e. heat protection systems, guide vans and turbine blades) in the gas turbine sector (Fig. 2).

The most well-known commercially available oxide fibres are the Nextel™ family from 3M™/US. Other oxide fibre manufacturers are Nitivy ALF™/JP and CeraFib/ODE. The focus is on alumina and aluminosilicate fibres; some contain dopants to obtain uniform and dense microstructures with small grain size (<0,5 µm).

Most of the commercial fibres are either not completely crystalline or contain a corundum phase: 3M™ Nextel™ 550 [1] and Nitivy ALF™ E3 80-20 [2, 3] consist of transitional alumina and amorphous silica; Nextel™ 720 contains two phases which are corundum and mullite [1, 4]. Both, the partially amorphous and corundum containing types, are prone to degradation of

Ralf Herborn, Arne Rüdiger,  
Peter Vierhaus  
Fraunhofer Institute for Silicate  
Research ISC / Center for High  
Temperature Materials  
97082 Würzburg, Germany

E-mail:  
ralf.herborn@isc.fraunhofer.de.com  
www.htl.fraunhofer.de

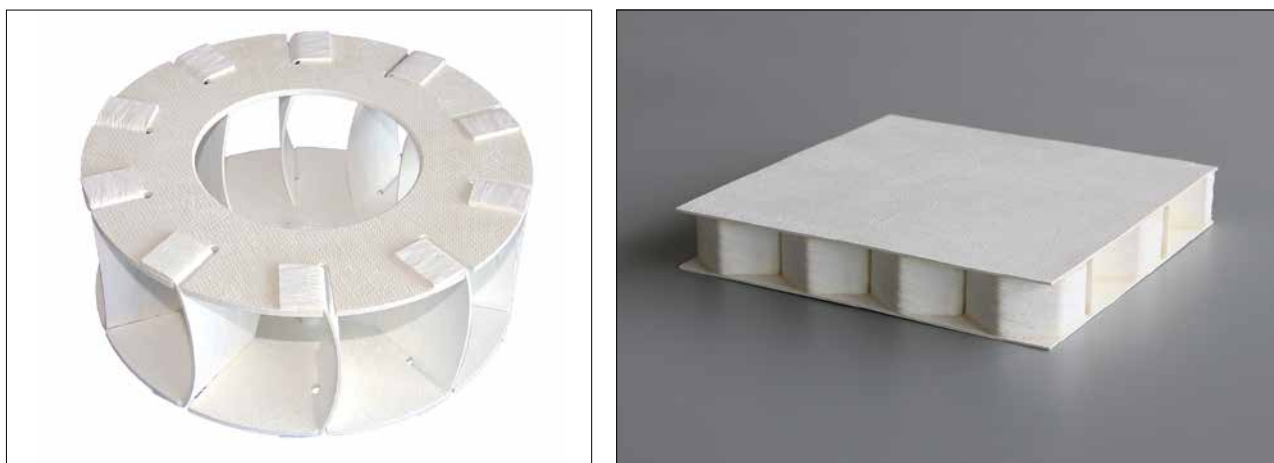


Fig. 2  
Joint fan wheel (l.), joined sandwich panel made from CMC (r.)

the mechanical properties when exposing the fibres to elevated temperatures. Mullite with the composition  $3\text{Al}_2\text{O}_3 \cdot 2\text{SiO}_2$  shows further outstanding properties such as low density, low thermal expansion and conductivity combined with excellent high temperature stability [5–7]. The most prominent oxide fibre types from 3M are Nextel™ 610 and Nextel™ 720. The Nextel™ 610 fibres consist of 98 mass-% alumina and have an excellent tensile strength of about 3000 MPa. The high strength of this fibre type is attained by

its fine microstructure of sub-micrometer alpha-alumina grains. The Nextel™ 720 fibre is actually the type with the most outstanding creep resistance and strength above 1100 °C and therefore the most preferred fibre for high temperature applications. Due to better high temperature properties of mullite compared to alpha-alumina, HTL decided in 2015 to start the development of a pure mullite fibre with 75 mass-% alumina and 25 mass-% silica. For synthesis of mullite fibres, the precursor par-

ticle size and homogeneity are crucial for the crystallization processes and mullite formation. In the literature, different approaches are described to develop mullite fibres. One way is the usage of monophasic gels. The basis is a uniform mix of Al- and Si-containing molecules at the atomic scale, which crystallize to mullite at low temperature of  $\approx 980$  °C [8–10]. Another way is the usage of colloidal gels. They are uniform mixtures of separated Al- and Si-containing clusters with diameters between 1–100 nm. The larger size of the



Fig. 3  
Synthesis of spin mass in a rotary evaporator

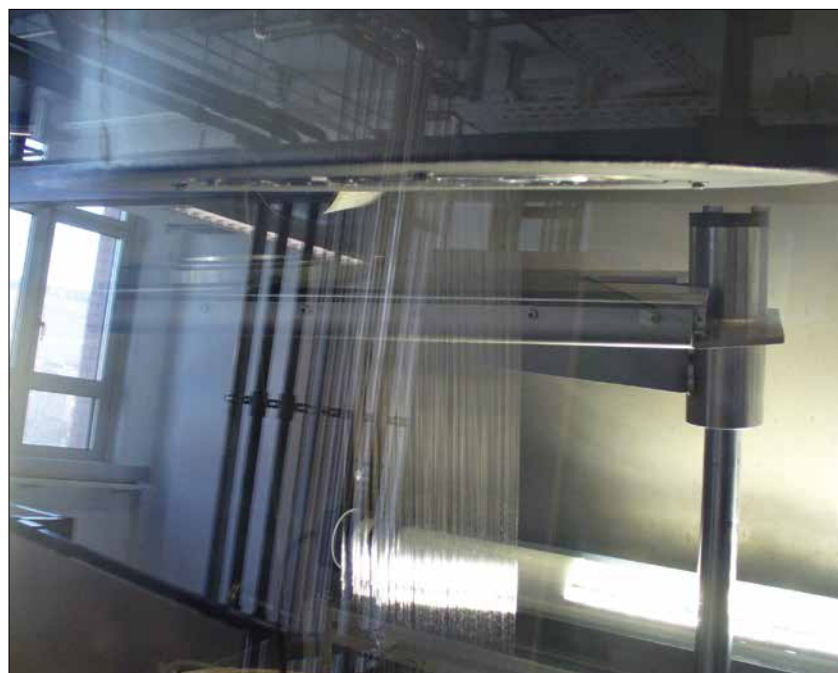


Fig. 4  
Spinning process at the HTL on a laboratory scale

colloidal particles results in initial formation of transitional aluminas and reaction with silica to mullite at higher temperatures between 1000–1350 °C [8, 11, 12]. Usually high raw material costs and low ceramic yields of both approaches are detrimental for commercialisation.

Taking into account the costs and ceramic yields of the used raw materials, HTL decided to use water-based cost-effective raw materials with high oxide contents for the fibre development. As aluminium precursor aluminumhydroxychloride (AHC) and colloidal silica as silicon precursor were used and mixed in a rotary evaporator (Fig. 3) to obtain a final composition of 75 : 25 mass-%  $\text{Al}_2\text{O}_3$  :  $\text{SiO}_2$  corresponding to 3 : 2 mullite. Water-based Polyvinyl Alcohol (PVA) was added as a spinning aid. The polymerization degree and concentration of PVA in the formulation is a crucial factor with regard to the spinning process. Reducing the water content of the formulation is essential to obtain the required rheology for high spinning quality. Approximately 40 mass-% of the formulation must be removed to receive a spinnable mass. Rheological preconditions for spinnability were evaluated by measurements of viscosity and viscoelastic properties with a rotation type rheometer (Anton Paar MCR501). The ideal window for best spinning results is a low shear (5/s) viscosity in the range of 100–400 Pa · s at room temperature. Viscoelastic properties like storage modulus  $G'$  and loss modulus  $G''$  are plotted as a function of frequency. Criteria for spinning are the course of  $G''$  and  $G'$  and their ratio  $\tan \delta$  when rotation frequency is increased.  $\tan \delta$  needs to be  $>1$  for successful spinning.

The fibre spinning process is done at room temperature in a laboratory plant (Fig. 4) that facilitates the manufacture of about 0,5 kg fibres per batch. Using a spin pump, the mass is pressed through different spinnerets with about 100 holes with diameters between 0,1–0,25 mm. The fibres pass through a vertical tube and are dried under controlled atmosphere using hot air with temperatures of 150–300 °C. After passing the tube, the fibres are finally wound onto a bobbin with speeds up to 500 m/min. The resulting fibre diameter varies between 15–20  $\mu\text{m}$ .

Thermal treatment and conversion to ceramic fibres is then done in two subse-

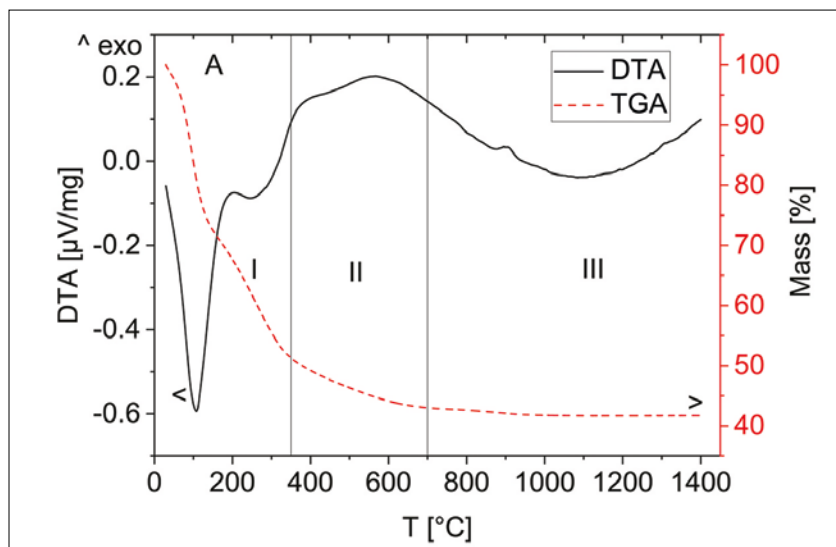


Fig. 5  
TGA and DTA analyses performed on the as-spun fibre

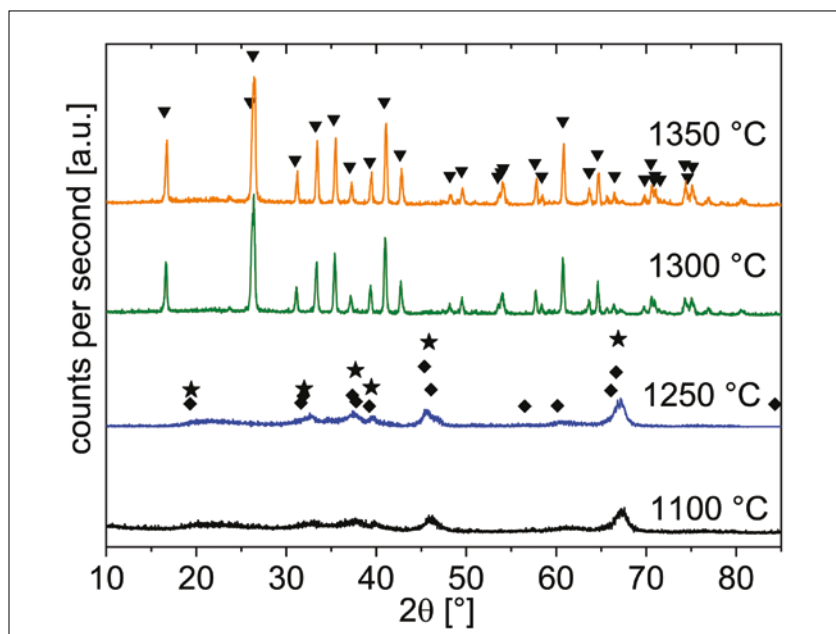


Fig. 6  
XRD patterns of fibres with mullite composition after heating to different temperatures: at 1100 °C and 1250 °C, fibres consist of transitional alumina (♦  $\eta$ -alumina, \*  $\gamma$ -alumina) and amorphous silica, from 1300 °C on, ▼-mullite is the main phase

quent steps. In the calcination step, the organic components are removed by using low heating rates (furnace: Heraeus M110). The calcination step ends at about 1100 °C with the formation of transition alumina phases. In the subsequent sintering step (Nabertherm HT 04/17), the transformation of the transition phases of alumina and silica to mullite takes place. Mass loss and phase changes were inves-

tigated by thermogravimetric and differential thermal analyses (TGA/DTA, Netzsch STA 449 C, Fig. 5).

The TGA curve of the as spun fibres reveals the critical temperatures of precursor decomposition. Three sections can be differentiated: (I) from RT up to 350 °C, where the largest mass loss takes place associated with the release of water vapour (the DTA curve shows two endo-

Tab. 1  
HTL fibre properties compared to commercially available oxide fibres

	Single Filament Tensile Strength [MPa]	Single Filament Tensile Young's Modulus [GPa]	Crystal Phases in Fibre [-]	Filament Diameter [ $\mu\text{m}$ ]	Density [ $\text{g}/\text{cm}^3$ ]
HTL transitional alumina grade	1600	170	$\gamma\text{-Al}_2\text{O}_3$ + amorphous $\text{SiO}_2$	8–12	2,4
HTL mullite grade	1400	200	mullite	8–12	3,0
3M™ Nextel™ 720	1500	230	mullite + $\alpha\text{-Al}_2\text{O}_3$	12–14	3,4
CeraFib75	1300	200	mullite	10–20	3,1
Nitivity ALF™ E3 (80–20)	1500	180	$\gamma\text{-Al}_2\text{O}_3$ + amorphous $\text{SiO}_2$	10	3,0

thermic peaks); (II) from 350–700 °C with release of residual water vapour, carbon dioxide and chlorine. The mass loss slows down, and beyond 700 °C, the weight is nearly constant and results in a ceramic yield of 42 mass-%. At the beginning of the third section (III), the evolution of the ceramic microstructure starts with the formation of transition alumina around 900 °C (exothermic peak).

The DTA curve gives a rough indication of the mullite crystallization temperature at about 1300 °C. X-ray Diffraction (XRD) provides complementary information to TGA/DTA in terms of ceramic phase formation, crystallization and crystallite sizes. Fig. 6 shows XRD-diagrams of a mullite precursor with a composition of 3 : 2 mullite. Temperature treatment of fibres at 1100 °C and 1250 °C results in

small and broad peaks indicating very small crystallites of transitional alumina. Mullite is formed between 1250–1300 °C directly from transitional alumina without intermediate  $\alpha$ -alumina formation. Since no clear difference is apparent for the 1300 °C and 1350 °C diffractogram, it is evident that mullite formation is complete at 1300 °C. The crystallite size of the mullite phase is larger compared to the transitional alumina phases giving rise to sharper mullite peaks. Crystallite size was calculated according to Scherrer's equation using the automatic calculation program of the software HighScore-Plus (Malvern Panalytical). Transitional alumina crystallite size was found to be around 10 nm, mullite crystallites are 60 nm for 1300 °C and 80 nm for 1350 °C.

Knowledge of mullite crystallization temperature is crucial for control of sintering temperatures and densification behaviour. Mullite derived from diphasic sol gel precursors densifies by viscous sintering of the amorphous silica rich phase prior to mullite formation [11, 13, 14]. Densification of the fibres stops when mullite crystallization occurs, which is attributed to the low diffusion rate of Al and Si species in mullite [11].

Consequently, the fibres have to be substantially dense, before mullite formation occurs, since further densification of mullite requires temperatures above 1500 °C, which would be detrimental for fibre properties. The sintered fibres have a final diameter between 8–12  $\mu\text{m}$ .

The mechanical single filament tensile strength and Young's modulus were meas-

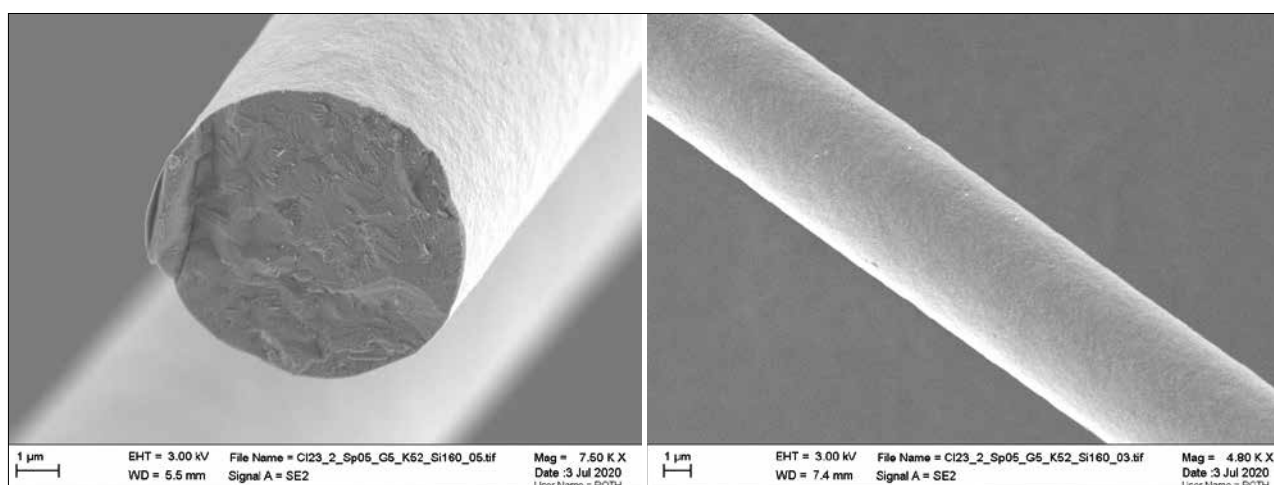


Fig. 7  
SEM micrographs of crystalline mullite fibres sintered at a maximum temperature of 1300 °C: fractured surface (l) and fibre surface (r.)

(Figs.: Fraunhofer-Center)

ured (Tab. 1) according to DIN EN 1007-4 (2004) using a single filament testing machine (Favimat+, Textechno). The filament diameter was automatically determined, measuring the fibres' resonance frequency, calculating the linear density and accordingly the filament diameter using the material density. Density measurement was conducted by pycnometry (Ultrapyc 1200e, Quantachrom/DE). Tab. 1 lists the mean values of 30 samples of filament diameter, Young's modulus and mechanical strength of two HTL fibre types (transitional grade and mullite grade) by comparison with three commercially available fibre types (3M™ Nextel™ 720, Nitivy ALF™ E3 80/20 and CeraFib75) as bench-

mark. The commercially available fibres were also tested at Fraunhofer Center HTL. Scanning Electron Microscopy (SEM, Zeiss Supra 25) is used to characterise fibre microstructures: grain sizes, pores and phase uniformity (Fig. 7). The fibre surfaces look fairly smooth. When regarding the fractured surface, a fine microstructure is recognised.

The next step concerning fibre development at the HTL will be the transfer from lab scale to pilot scale, demonstrating manufacturing capability.

A pilot plant with 500–2000 filaments and a yearly capacity of up to 1000 kg of oxide fibres is currently under construction at the HTL site in Bayreuth, including calcination

and sintering facilities. This R&D pilot line for developing oxide ceramic fibres will start operation in the year 2021. This line will have a theoretical 24/7 capacity up to yearly 1 t, based on a sol-gel dry-spinning process with up to 2000 filaments per roving under controlled atmosphere, followed by a batch calcination and continuous sintering process for endless rovings with lengths of 200–500 m/bobbin.

#### Acknowledgements

The financial support from the Bavarian Ministry of Economic Affairs and Media, Energy and Technology and the Deutsche Bundesstiftung Umwelt (DBU) is greatly acknowledged.

#### References

- [1] 3M: Nextel™ Ceramic Textiles Technical Notebook
- [2] Hiltex Semi Products: Hiltex ALF – Hiltex boron-free continuous alumina-silica fibre. 1525 RG West-Knollendam, The Netherlands
- [3] Wang, Y.; et al.: Microstructure and room temperature mechanical properties of mullite fibres after heat-treatment at elevated temperatures. *Mater. Sci. Engin. A* **578** (2013) 287–293
- [4] Wilson, D.M.; Visser, L.R.: High performance oxide fibres for metal and ceramic composites. *Composites Part A* **32** (2001) 1143–1153
- [5] Schneider, H.; Fischer, R.X.; Schreuer, J.: Mullite: Crystal structure and related properties. *J. Amer. Ceram. Soc* **98** (2015) [10] 2948–2967
- [6] Anggono, J.: Mullite Ceramics: Its Properties, Structure, and Synthesis. *Jurnal Teknik Mesin* **7** (2005) [1] 1–10
- [7] Aksay, I.A.; et al.: Mullite for structural, electronic, and optical applications. *J. Amer. Ceram. Soc.* **74** (1991) [10] 2343–2358
- [8] Cividanis, L.S.; et al.: Review of mullite synthesis routes by sol-gel method. *J Sol-Gel Sci. Technol.* **55** (2010) 111–125
- [9] Yoldas, B.E.; Partlow, D.P.: Formation of mullite and other alumina-based ceramics via hydrolytic polycondensation of alkoxides and resultant ultra- and microstructural effects. *J. Mater. Sci.* **23** (1988) 1895–1900
- [10] Cassidy, D.J.; et al.: The effect of precursor chemistry on the crystallisation and densification of sol-gel derived mullite gels and powders. *J. Sol-Gel Sci. Technol.* **10** (1997) 19–30
- [11] Fahrenholtz, W.G.; et al.: Effect of precursor particle size on the densification and crystallization behavior of mullite. *J. Amer. Ceram. Soc.* **76** (1993) [2] 433–437
- [12] Kong, L.B.; et al.: Mullite phase formation in oxide mixtures in the presence of  $Y_2O_3$ ,  $La_2O_3$  and  $CeO_2$ . *J. Alloys Compd.* **372** (2004) 290–299
- [13] Ivankovic, H.; et al.: Correlation of the precursor type with densification behavior and microstructure of sintered mullite ceramics. *J. Europ. Ceram. Soc.* **23** (2003) 283–292
- [14] Hong, S.H.; Cermignani, W.; Messing, G.L.: Anisotropic grain growth in seeded and  $B_2O_3$ -doped diphasic mullite gels. *J. Europ. Ceram. Soc.* **16** (1996) 133–141